

# Response of Plasmas to Tungsten Pellet Injection in Neutral Beam Heated Discharges in Large Helical Device<sup>\*)</sup>

Tetsutarou OISHI<sup>1,2)</sup>, Shigeru MORITA<sup>1,2)</sup>, Xianli HUANG<sup>1)</sup>, Yang LIU<sup>2)</sup>, Motoshi GOTO<sup>1,2)</sup> and the LHD Experiment Group<sup>1)</sup>

<sup>1)</sup>National Institute for Fusion Science, National Institutes of Natural Sciences, 322-6 Oroshi-cho, Toki 509-5292, Japan

<sup>2)</sup>Department of Fusion Science, SOKENDAI (Graduate University for Advanced Studies), 322-6 Oroshi-cho, Toki 509-5292, Japan

(Received 28 December 2017 / Accepted 19 March 2018)

Response of plasmas in Large Helical Device (LHD) to the tungsten pellet injection depends on both the total port-through power of the neutral beam injection (NBI) for heating,  $P_{\text{NBI}}$ , and the line-averaged electron density,  $n_e$ . The plasma can be sustained in the range of high  $P_{\text{NBI}}$  and low  $n_e$  while it collapses in the range of low  $P_{\text{NBI}}$  and high  $n_e$ . When the number of tungsten atoms enclosed in a pellet,  $N_W$ , is small, plasma can survive in low  $P_{\text{NBI}}$  and high  $n_e$  range. Parameter space for plasma sustainment after the pellet injection is limited to lower  $n_e$  range in more outward-shifted magnetic configuration.  $n_e < 4.0 \times 10^{13} \text{ cm}^{-3}$  and  $N_W < 1.2 \times 10^{18}$  for  $R_{\text{ax}} = 3.60 \text{ m}$ ,  $n_e < 3.0 \times 10^{13} \text{ cm}^{-3}$  and  $N_W < 8.7 \times 10^{16}$  for  $R_{\text{ax}} = 3.75 \text{ m}$ , and  $n_e < 2.0 \times 10^{13} \text{ cm}^{-3}$  and  $N_W < 3.1 \times 10^{16}$  for  $R_{\text{ax}} = 3.90 \text{ m}$  are appropriate parameter ranges for the plasma sustainment. This suggests that robustness against tungsten injection depends on the magnetic configurations.

© 2018 The Japan Society of Plasma Science and Nuclear Fusion Research

Keywords: impurity pellet, plasma spectroscopy, magnetically confined fusion, impurity transport, tungsten

DOI: 10.1585/pfr.13.3402031

## 1. Introduction

Tungsten is regarded as a leading candidate material for the plasma facing components (PFCs) in ITER and future fusion reactors because of its high melting point, low sputtering yield, and low tritium retention [1–3]. One of the major concerns regarding the tungsten PFC is that the tungsten ion causes a large radiation loss due to its large atomic number of  $Z = 74$  when it contaminates plasmas. Considering transport processes of tungsten impurity in plasma confinement devices with tungsten PFCs, firstly neutral tungsten atoms are sputtered and released from the divertor plates. The tungsten ions in lower ionization stages are transported through the edge plasmas and finally the tungsten ions in higher ionization stages are accumulated in the core plasmas. Therefore, diagnostics for tungsten ions covering from low to high ionization stages are necessary for the comprehensive understanding of the tungsten transport.

Spectroscopic studies for emissions released from tungsten ions have been intensively conducted in the Large Helical Device (LHD) for contribution to the tungsten transport study in tungsten-divertor fusion devices and for the expansion of experimental database of tungsten line emissions. Tungsten ions are distributed in the LHD plasma by injecting a pellet consisting of a small piece of tungsten metal wire. In order to perform the tungsten

injection experiment successfully, we must avoid plasma collapse by energy losses due to ionization and radiation of tungsten ions. Therefore, it is important to investigate responses of the plasmas to the pellet injection and to survey appropriate experimental conditions to sustain plasmas even though the tungsten ions are distributed in the plasmas. In this study, the response of the plasmas to the pellet injection is summarized, which depends on both the total port-through power of the neutral beam injection (NBI) for heating,  $P_{\text{NBI}}$ , and the line-averaged electron density,  $n_e$ .

## 2. Tungsten Pellet Injection Experiments in LHD

Figure 1 illustrates a schematic drawing of vacuum ul-

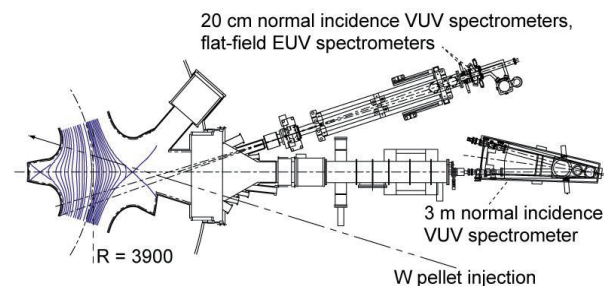


Fig. 1 Schematic drawing of VUV and EUV spectrometers used for the tungsten spectroscopy in LHD. Top view of magnetic surfaces ( $R_{\text{ax}} = 3.6 \text{ m}$ ), optical axis of the spectrometers, and incident orbit of impurity pellet are illustrated together.

author's e-mail: oishi@nifs.ac.jp

<sup>\*)</sup> This article is based on the presentation at the 26th International Toki Conference (ITC26).

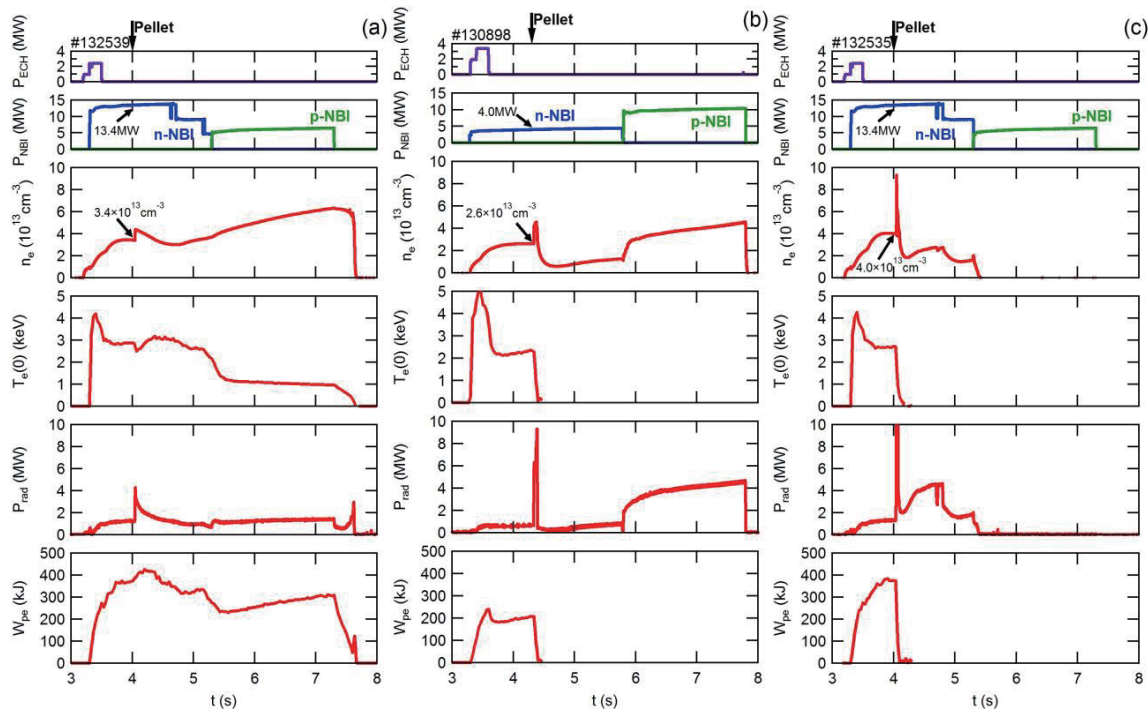


Fig. 2 Injected power of ECH,  $P_{ECH}$ , and NBI,  $P_{NBI}$ , line-averaged electron density,  $n_e$ , central electron temperature,  $T_{e0}$ , total radiation power,  $P_{rad}$ , and electron kinetic energy,  $W_{pe}$ , in typical waveforms of W pellet injection experiments in LHD. The number of atoms enclosed in a pellet,  $N_W$ , is  $8.7 \times 10^{16}$ . (a) Plasmas can be sustained after the tungsten pellet injection with high  $P_{NBI}$  and low  $n_e$ . Plasmas are collapsed just after the pellet injection due to (b) low  $P_{NBI}$  or (c) high  $n_e$  at the pellet injection.

traviolet (VUV) and extreme ultraviolet (EUV) spectrometers used for the tungsten spectroscopy in LHD [4–6]. Top view of magnetic surfaces (position of the magnetic axis  $R_{ax} = 3.6$  m), optical axis of the spectrometers, and incident orbit of impurity pellet are shown together. LHD has the major/minor radii of 3.6/0.64 m in the standard configuration with maximum plasma volume of 30 m<sup>3</sup> and toroidal magnetic field of 3 T. The coil system consists of a set of two continuous superconducting helical coils with poloidal pitch number of 2 and toroidal pitch number of 10 and three pairs of superconducting poloidal coils. Tungsten ions are distributed in the LHD plasma by injecting a pellet consisting of a small piece of tungsten metal wire enclosed by a carbon or polyethylene tube. The length and diameter of a W wire can be selected in ranges of 0.5 ~ 1.0 mm and 0.02 ~ 0.2 mm, respectively [7]. Then a pellet is made up of approximately  $1 \times 10^{16} \sim 2 \times 10^{18}$  W atoms and accelerated by pressurized He gas of 10 ~ 20 atm. The pellet injection orbit is located on the midplane of the plasma having a 12° angle from the normal to the toroidal magnetic axis [8]. By using the pellet injection and spectroscopy system, we have already identified tungsten line emissions of WIV–WVII in the VUV range [9, 10] and WXLV and WXLVI in the EUV range [11]. Identification study on the unresolved transition array consisting of WXXV–WXXIX lines also has been progressed recently [12].

Figure 2 (a) shows a typical waveform of the tungsten

pellet injection experiment with hydrogen discharge with magnetic axis position,  $R_{ax}$ , of 3.60 m at toroidal magnetic field,  $B_t$ , of  $-2.75$  T. Here, the minus sign of  $B_t$  means inverse direction, i.e., counter-clockwise direction. The plasma was initiated by the electron cyclotron heating, and further heated by the neutral hydrogen beams. At the timing of the tungsten pellet injection of 4.0 s,  $P_{NBI}$  is 13.4 MW and  $n_e$  is  $3.4 \times 10^{13}$  cm<sup>-3</sup>. The length and diameter of a W wire is 0.7 mm and 0.05 mm, respectively. Then, the number of atoms enclosed in a pellet,  $N_W$ , is  $8.7 \times 10^{16}$ . After the pellet injection, the central electron temperature,  $T_{e0}$ , quickly decreases while  $n_e$  increases. Thereafter  $T_{e0}$  and the plasma stored energy evaluated from the kinetic energy of electrons,  $W_{pe}$ , start to increase due to continuous neutral beam heating.

We have found that plasmas can be sustained after the tungsten pellet injection with high  $P_{NBI}$  and low  $n_e$  as shown in Fig. 2 (a). However, depending on experimental conditions, plasmas collapse suddenly just after the pellet injection. Figures 2 (b) and (c) show waveforms of the collapse shots with low  $P_{NBI}$  of 4.0 MW and high  $n_e$  of  $4.0 \times 10^{13}$  cm<sup>-3</sup> at the pellet injection, respectively. In these cases, the neutral beam heating cannot afford to sustain plasmas with high power loss by ionization and radiation due to high electron density. It has been already known that the allowable density rise due to a pellet injection without plasma collapse decreases with the atomic number of the injected atom [13]. When the hydrogen pellets are in-

jected, the plasma can be sustained with the density rise close to  $1.0 \times 10^{14} \text{ cm}^{-3}$ . On the other hand, typical density rise without collapse for  $N_W = 8.7 \times 10^{16}$  is  $1.0 \times 10^{13} \text{ cm}^{-3}$  as shown in Fig. 2 (a).

### 3. Parameter Range Survey for Plasma Sustainment after the Tungsten Pellet Injection

As shown in Fig. 2, success in the tungsten pellet in-

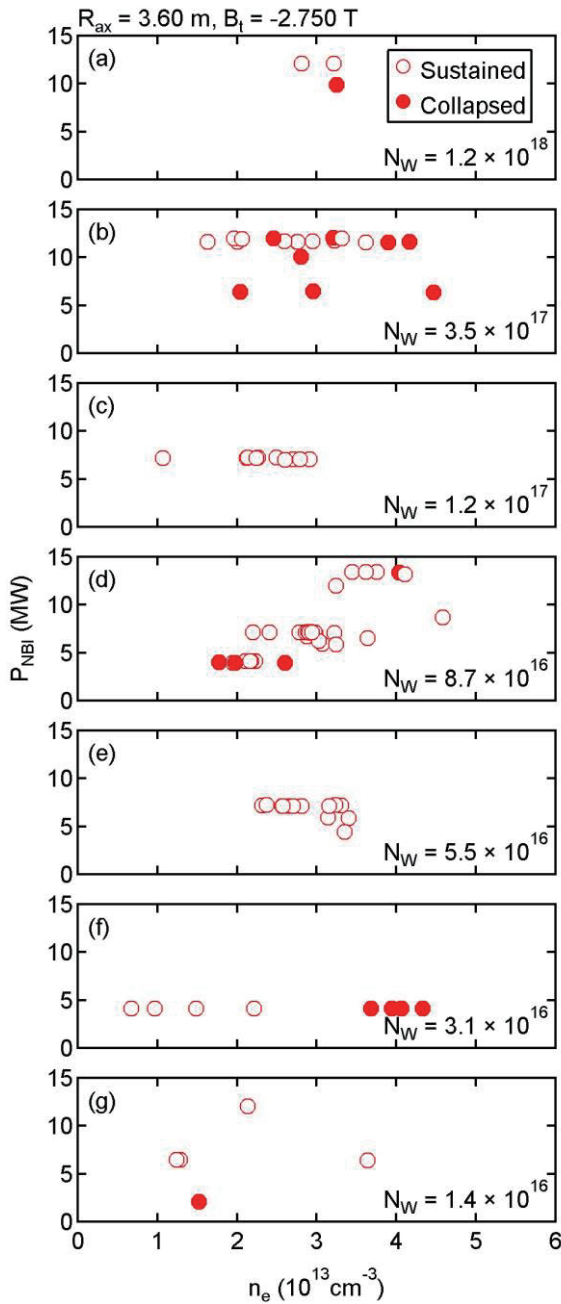


Fig. 3 Results of the tungsten pellet injection as a function of  $P_{\text{NBI}}$  and  $n_e$ , with  $R_{\text{ax}} = 3.60 \text{ m}$  for several kinds of numbers of tungsten atoms enclosed in a pellet,  $N_W$ . Open circle and closed circle mean sustained and collapsed shot, respectively.

jection depends on both the NBI heating power and the electron density. Figure 3 shows the results of the pellet injection as a function of  $P_{\text{NBI}}$  and  $n_e$  with  $R_{\text{ax}} = 3.60 \text{ m}$ . We can select  $N_W$  by changing the size of the pellet. In Fig. 3, open circle and closed circle means sustained and collapsed shots, respectively. The pellet injection successes in the range of high  $P_{\text{NBI}}$  and low  $n_e$  while it fails in the range of low  $P_{\text{NBI}}$  and high  $n_e$ . Roughly speaking,  $n_e < 4.0 \times 10^{13} \text{ cm}^{-3}$  is an appropriate density range for the cases with relatively large pellets, i.e.  $N_W = 1.2 \times 10^{18}$  or  $3.5 \times 10^{17}$  as shown in Figs. 3 (a) and (b), if  $P_{\text{NBI}}$  is higher than 10 MW. When  $N_W$  is small, plasma can be sustained in low  $P_{\text{NBI}}$  range ( $\sim 5 \text{ MW}$ ) as shown in Figs. 3 (c-g).

We conducted the experiments with three kinds of  $R_{\text{ax}}$ , 3.60 m, 3.75 m, and 3.90 m. Large  $R_{\text{ax}}$  value means that a position of the magnetic axis is shifted outward. Figures 4 and 5 shows the sustained and collapsed shots with  $R_{\text{ax}} = 3.75 \text{ m}$  and 3.90 m, respectively. Parameter space for the sustained shot is limited to lower  $n_e$  range in the more outward-shifted configuration.  $n_e < 3.0 \times 10^{13} \text{ cm}^{-3}$  and  $N_W < 8.7 \times 10^{16}$  for  $R_{\text{ax}} = 3.75 \text{ m}$  and  $n_e < 2.0 \times 10^{13} \text{ cm}^{-3}$  and  $N_W < 3.1 \times 10^{16}$  for  $R_{\text{ax}} = 3.90 \text{ m}$  are appropriate parameter ranges for the plasma sustainment.

Figure 6 shows the dependence of  $T_{e0}$  and  $W_{\text{pe}}$  on  $n_e$  with  $R_{\text{ax}} = 3.60 \text{ m}$ , 3.75 m, and 3.90 m for the shots with  $10 \text{ MW} < P_{\text{NBI}} < 15 \text{ MW}$  and  $N_W = 3.5 \times 10^{17}$ . Open and closed symbols mean sustained and collapsed shots, respectively. As shown in Fig. 6, the electron temperature is lower than that in the inward-shifted configuration under the same electron density and the heating power in the outward-shifted magnetic configuration, which results in smaller plasma stored energy in the outward-shifted configuration. Therefore, one of the reasons for the depen-

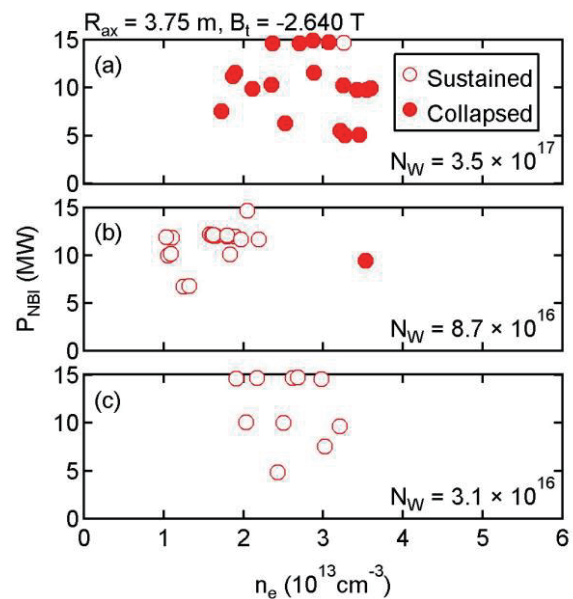


Fig. 4 Results of the tungsten pellet injection as a function of  $P_{\text{NBI}}$  and  $n_e$ , with  $R_{\text{ax}} = 3.75 \text{ m}$ .

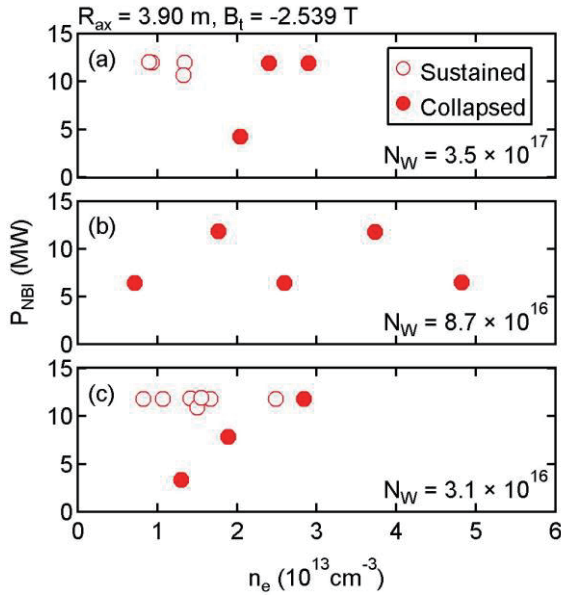


Fig. 5 Results of the tungsten pellet injection as a function of  $P_{\text{NBI}}$  and  $n_e$ , with  $R_{\text{ax}} = 3.90$  m.

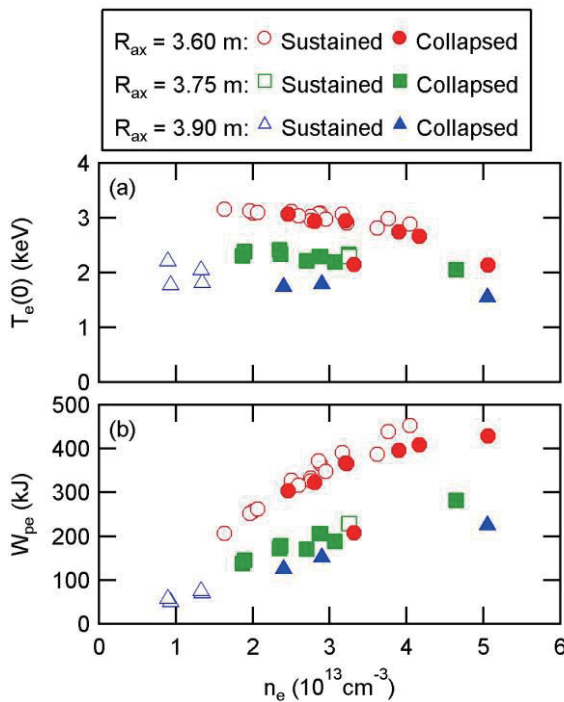


Fig. 6 Dependence of (a)  $T_{e0}$  and (b)  $W_{\text{pe}}$  on  $n_e$  with  $R_{\text{ax}} = 3.60$  m,  $3.75$  m, and  $3.90$  m for the shots with  $10 \text{ MW} < P_{\text{NBI}} < 15 \text{ MW}$  and  $N_W = 3.5 \times 10^{17}$ . Open and closed symbols mean sustained and collapsed shots, respectively.

dence of acceptable amount of the tungsten atoms on the magnetic configuration is that the plasma cannot be sustained by the smaller stored energy against the energy loss by the tungsten injection in the outward-shifted configuration. The response of radial profiles of plasma parameters to the pellet injection, the radial position of pellet deposition, and the density limit without pellet injection should be also compared between different magnetic configurations in the future studies in order to clarify the difference in the acceptable amount of the tungsten atoms.

## 4. Summary

Response of the LHD plasmas to the tungsten pellet injection depends on both  $P_{\text{NBI}}$  and  $n_e$ . The plasma can be sustained in the range of high  $P_{\text{NBI}}$  and low  $n_e$  while it collapses in the range of low  $P_{\text{NBI}}$  and high  $n_e$ . When  $N_W$  is small, plasma can survive in low  $P_{\text{NBI}}$  and high  $n_e$  range. Parameter space for plasma sustainment after the pellet injection is limited to lower  $n_e$  range in more outward-shifted magnetic configuration. This suggests that robustness against tungsten injection depends on the magnetic configurations.

## Acknowledgement

The authors thank all the members of the LHD team for their cooperation with the LHD operation. This work is partially conducted under the LHD project financial support (NIFS14ULPP010, NIFS15ULPP038). This work was also supported by Grant-in-Aid for Young Scientists (B) (26800282, 17K14426) and partially supported by the JSPS-NRF-NSFC A3 Foresight Program in the Field of Plasma Physics (NSFC: No.11261140328, NRF: No.2012K2A2A6000443).

- [1] D.W. Ignat *et al.*, Nucl. Fusion **39**, 2137 (1999).
- [2] R. Neu *et al.*, Nucl. Fusion **45**, 209 (2005).
- [3] J. Roth *et al.*, Plasma Phys. Control. Fusion **50**, 103001 (2008).
- [4] T. Oishi *et al.*, Appl. Opt. **53**, 6900 (2014).
- [5] M.B. Chowdhuri *et al.*, Rev. Sci. Instrum. **78**, 023501 (2007).
- [6] M.B. Chowdhuri, S. Morita and M. Goto, Appl. Opt. **47**, 135 (2008).
- [7] X.L. Huang *et al.*, Rev. Sci. Instrum. **85**, 11E818 (2014).
- [8] H. Nozato *et al.*, Rev. Sci. Instrum. **74**, 2032 (2003).
- [9] T. Oishi *et al.*, Phys. Scr. **91**, 025602 (2016).
- [10] T. Oishi *et al.*, Plasma Fusion. Res. **10**, 3402031 (2015).
- [11] S. Morita *et al.*, AIP Conference Proceedings **1545**, 143 (2013), Proceedings of ICAMDATA-2012, Gaithersburg, 30 Sept.–4 Oct. 2012.
- [12] Y. Liu *et al.*, J. Appl. Phys. **122**, 233301 (2017).
- [13] S. Morita *et al.*, Plasma Sci. Technol. **13**, 290 (2011).